



HAL
open science

Mechanism of differential control of NMDA receptor activity by NR2 subunits

Marc Gielen, Beth Siegler Retchless, Laetitia Mony, Jon W Johnson, Pierre Paoletti

► **To cite this version:**

Marc Gielen, Beth Siegler Retchless, Laetitia Mony, Jon W Johnson, Pierre Paoletti. Mechanism of differential control of NMDA receptor activity by NR2 subunits. *Nature*, 2009, <http://www.nature.com/nature/journal/v459/n7247/full/nature07993.html>. <10.1038/nature07993>. <hal-01145441>

HAL Id: hal-01145441

<https://hal.science/hal-01145441v1>

Submitted on 24 Apr 2015

HAL is a multi-disciplinary open access archive for the deposit and dissemination of scientific research documents, whether they are published or not. The documents may come from teaching and research institutions in France or abroad, or from public or private research centers.

L'archive ouverte pluridisciplinaire **HAL**, est destinée au dépôt et à la diffusion de documents scientifiques de niveau recherche, publiés ou non, émanant des établissements d'enseignement et de recherche français ou étrangers, des laboratoires publics ou privés.



HAL Authorization

Published in final edited form as:

Nature. 2009 June 4; 459(7247): 703–707. doi:10.1038/nature07993.

Mechanism of differential control of NMDA receptor activity by NR2 subunits

Marc Gielen¹, Beth Siegler Retchless², Laetitia Mony¹, Jon W. Johnson², and Pierre Paoletti¹

¹Laboratoire de Neurobiologie, Ecole Normale Supérieure, CNRS 46 rue d'Ulm, 75005 Paris, France

²Department of Neuroscience, University of Pittsburgh, A210 Langely Hall, Pittsburgh, PA 15260, USA

Abstract

NMDA receptors (NMDARs) are a major class of excitatory neurotransmitter receptors in the central nervous system. They form glutamate-gated ion channels highly permeable to calcium that mediate activity-dependent synaptic plasticity¹. NMDAR dysfunction is implicated in multiple brain disorders, including stroke, chronic pain and schizophrenia². NMDARs exist as multiple subtypes with distinct pharmacological and biophysical properties largely determined by the type of NR2 subunit (NR2A–NR2D) incorporated in the heteromeric NR1/NR2 complex^{1,3,4}. A fundamental difference between NMDAR subtypes is their channel maximal open probability (P_o), which spans a 50-fold range from ~0.5 for NR2A-containing receptors to ~0.01 for NR2C- and NR2D-containing receptors; NR2B-containing receptors having an intermediate value (~0.1)^{5–9}. These differences in P_o confer unique charge transfer capacities and signaling properties on each receptor subtype^{4,6,10,11}. The molecular basis for this profound difference in activity between NMDAR subtypes is unknown. Here we demonstrate that the subunit-specific gating of NMDARs is controlled by the region formed by the NR2 N-terminal domain (NTD), an extracellular clamshell-like domain previously shown to bind allosteric inhibitors^{12–15}, and the short linker connecting the NTD to the agonist-binding domain (ABD). Subtype specificity of NMDAR P_o largely reflects differences in the spontaneous (ligand-independent) equilibrium between open-cleft and closed-cleft conformations of the NR2-NTD. This NTD-driven gating control also impacts pharmacological properties, by setting the sensitivity to the endogenous inhibitors zinc and protons. Our results provide a proof-of-concept for a drug-based bidirectional control of NMDAR activity using molecules acting either as NR2-NTD “closers” or “openers” promoting receptor inhibition or potentiation, respectively.

Keywords

glutamate receptors; NMDA; gating; channel; synapse; allosteric modulation

We first explored the role of the NR2-NTD in the difference of P_o between NR1/NR2A and NR1/NR2B receptors by evaluating the effect of deleting the entire NR2-NTD on receptor activity. We estimated P_o using a method based on the covalent modification of a cysteine introduced in the NR1 subunit (NR1-A652C), which locks open the NMDAR channel¹⁶. Although this method does not give access to the absolute P_o of receptors containing the wild-type (wt) NR1 subunit, it can report relative differences in channel activity¹⁷. Indeed,

the extent to which the sulfhydryl-modifying reagent MTSEA potentiates NMDAR currents is inversely related to the channel P_o . MTSEA potentiated currents carried by NR1-A652C/NR2B receptors to a much greater extent than currents of NR1-A652C/NR2A receptors (Fig. 1a&d), consistent with the much lower P_o of NR2B-containing receptors compared to NR2A-containing receptors^{5,6,17}. In contrast, MTSEA-induced potentiations of NR1-A652C/NR2A- Δ NTD and NR1-A652C/NR2B- Δ NTD receptors were indistinguishable (Fig. 1b&d) indicating equal receptor activities. However, receptors incorporating chimeric NR2A-(2B NTD) or NR2B-(2A NTD) subunits displayed MTSEA-induced potentiations similar to those of the parental NR2 subunits, indicating that swapping the NTDs alone did not exchange the P_o (Fig. 1d). We therefore swapped both the NTD and the highly divergent short (14 residues) linker segment that connects the NTD to the ABD (Fig. S1). Remarkably, NR1-A652C/NR2A-(2B NTD+L) and NR1-A652C/NR2B-(2A NTD+L) responses supported levels of MTSEA potentiation closer to those of NR2Bwt-containing and NR2Awt-containing receptors, respectively (Fig. 1c&d). Direct measurement of channel activity using single-channel recordings confirmed this exchange of P_o (Fig. 1e and Fig S2).

We next extended the analysis to the NR2D subunit. MTSEA-induced potentiations of NR2D-containing receptors were considerable (~300-fold), reflecting the very low P_o of NR1/NR2D receptors (Fig. 1d). Deleting the NR2D-NTD resulted in a 4-fold decrease in MTSEA potentiation, indicative of a markedly increased P_o (Fig. 1d). This gain-of-function phenotype could be reinforced by grafting on NR2D- Δ NTD the NTD+linker region of the high- P_o subunit NR2A. Reversibly, receptors containing the chimeric NR2A-(2D NTD+L) subunit displayed 17-fold higher MTSEA-potentiation than NR2Awt-containing receptors, suggestive of a much lower P_o (Fig. 1d). Thus, the low P_o of the NR2D-containing receptors is also set by the NR2-NTD.

Since P_o estimation using MTSEA relies on a mutated NR1 subunit (NR1-A652C), we checked that the effects observed did not depend on this mutation. We used the time constant of inhibition by MK-801, an NMDAR open-channel blocker, as an alternative method to assess P_o ^{5,18}. Consistent with the higher P_o of NR2A- vs NR2B-containing receptors, MK-801 inhibited wt NR1/NR2A receptors significantly faster than wt NR1/NR2B receptors (Fig. S3a&b). Deleting the NR2-NTDs abolished this difference (Fig. S3b). While swapping the NR2-NTD alone did not exchange MK-801 time constants, incorporating the NTD-ABD linker achieved almost complete transfer (Fig. S3a&b). As expected, the onset of MK-801 inhibition at wt NR1/NR2D receptors was much slower than at NR2A- or NR2B-containing receptors. Deleting the NR2D-NTD or replacing the NTD+linker region of NR2D by that of NR2A strongly accelerated MK-801 inhibition, indicative of a much increased P_o (Fig. 1f and Fig S3c). Conversely, MK-801 inhibition of receptors incorporating NR2A-(2D NTD+L) was 15-fold slower than at NR2Awt-containing receptors (Fig. S3b). Together with the MTSEA experiments, these results demonstrate that the NR2-NTD+linker region is a major determinant of the NR2 subunit-specific activity of NMDARs.

We next investigated the mechanism by which a distal domain, the NR2-NTD, influences channel activity. Previous studies on allosteric inhibition of NMDARs by NR2-NTD ligands, such as zinc and ifenprodil, suggested that these ligands bind the NTD cleft and promote its closure^{12,15,19}. This in turn leads to receptor inhibition through disruption of the NR1/NR2 ABD dimer interface, resembling the mechanism underlying AMPAR desensitization^{20–22}. Since the NTD can adopt at least two conformations, a ligand-free open state and a ligand-bound closed state, we hypothesized that the NTD-driven control of P_o might result from spontaneous oscillations of the NR2-NTD between an open-cleft conformation, favoring channel opening, and a closed-cleft conformation, favoring pore

closure. Such ligand-independent oscillations have been observed in several clamshell-like proteins, including the bacterial maltose-binding-protein²³ (MBP) and the GABA-B receptor²⁴. To test this hypothesis, we introduced cysteines in the NR2-NTD cleft to lock open the NR2-NTDs using thiol-reactive MTS reagents. Based on 3D models, we first introduced a cysteine deep in the cleft of the NR2B-NTD by mutating the hinge residue NR2B-Y282, whose side chain points toward the cleft entrance (Fig. 2a and ref²⁵). Application of the positively charged MTSEA potentiated NR1wt/NR2B-Y282C receptors but not control NR1wt/NR2B-Y282S receptors (Fig. 2b). Strikingly, using MTS compounds of same valence but different sizes, we observed that the larger the MTS, the greater the potentiation (Fig. 2b&c). Comparison of the rates of MK-801 inhibition before and after MTS treatment together with direct measurement of single-channel activity revealed that current potentiations reflected an increase in P_o (Fig. S4 and S5). Sensitivity to glycine (binding the NR1-ABD) was unaltered by MTS treatment, while sensitivity to glutamate (binding the NR2-ABD) was slightly decreased (Fig. S6), as expected from the known allosteric interaction between the NR2 NTD and ABD²⁶. Interestingly, MTS action was significantly faster on resting than activated receptors (Fig. S7), further arguing for a facilitated opening of the NR2-NTD when the ABD is open. Altogether, these results show that trapping open the NR2-NTD enhances receptor activity. They also indicate that the NTD of NR2B-Y282C is not permanently open (since there was a potentiating effect of the MTS compounds) nor closed (since the introduced cysteine was accessible to MTS), but rather alternates between open and closed conformations, the latter favoring pore closure.

Because NR2B-Y282 is a large residue, we considered the possibility that its mutation into a small residue (cysteine or serine) may have artificially increased the flexibility of the NTD hinge, favoring NTD closure. Indeed, such mutations strongly reduced receptor activity (Fig. S8). This effect highlights the unsuspected role of the NR2-NTD hinge in shaping NMDAR P_o , reminiscent of the critical role of the MBP hinge in controlling the apparent maltose affinity²⁷. To extend our conclusion of spontaneous NR2-NTD oscillations to receptors with unaltered gating properties, we targeted NR2B-NTD H127, since its mutation into cysteine minimally affects receptor activity (Fig. S8). MTS compounds still potentiated NR1wt/NR2B-H127C receptors (but not control NR1wt/NR2B-H127A receptors) in a size-dependent manner. However, potentiations were considerably smaller than with NR1wt/NR2B-Y282C receptors (Fig. 2c and Fig S9a). Two reasons may explain this difference: higher basal P_o of NR1wt/NR2B-H127C receptors, and wider opening of the NTD at MTS-modified NR2B-Y282C subunits because of the deeper location in the cleft of Y282. Overall, these results provide the important new information that spontaneous oscillations of the NR2B-NTD contribute to the low P_o of wt NR1/NR2B receptors.

We then tested the prediction that the high P_o of NR2A-containing receptors results from the NR2A-NTD preferring the open conformation. As for NR2B, we found the P_o of NR2A-containing receptors to be significantly reduced by the mutation of NR2A-Y281 into small residues (Fig. S8). A potentiating component was also observed at receptors containing NR2A-Y281C during treatment by MTS compounds, but not at control NR2A-Y281A receptors. However, MTS-induced potentiations were much smaller than at NR2B-Y282C receptors and were independent of MTS size (Fig. 2c and Fig S9b), suggesting that the NR2A-NTD is much less sensitive to steric hindrance than the NR2B-NTD. In addition, no potentiation was observed at NR2A-H128C receptors even with the large MTS-PtrEA (Fig. 2c and Fig S9b). This is consistent with the NR2A-NTD spending most of its time in an open-cleft conformation, thus contributing to the relatively high P_o of NR2A-containing receptors.

Our results on chimeric NR2 subunits, showing that the NTD-ABD linker is required for the differential influence of the NR2-NTD on receptor P_o , raised the possibility that this

element is also crucial during allosteric modulation of NMDARs by NTD-ligands. NR2A-NTD forms a high affinity zinc inhibitory site^{12–14}; accordingly, NR1wt/NR2D-(2A NTD +L) receptors were highly sensitive to zinc (Fig. 3a). NR1wt/NR2B-(2A NTD) receptors are also highly sensitive to zinc. Surprisingly, zinc appears much more potent at these receptors than at wt NR1/NR2A receptors (Fig. 3a), suggesting that the NR2B NTD-ABD linker facilitates NTD-cleft closure. Increasing the chimera length to incorporate the NR2A NTD-ABD linker almost completely restored NR2Awt-like zinc sensitivity (Fig. 3a). This highlights again the importance of the NTD-ABD linker for the communication between the NTD and the gating machinery.

Proton is another allosteric modulator that differentially inhibits NMDAR subtypes¹. In contrast with the zinc sensor, the proton sensor is thought to be closely associated with the channel gate²⁸. Unexpectedly, deleting the NR2-NTDs fully abolished the difference in pH sensitivity between wt NR1/NR2A and NR1/NR2B receptors (Fig. 3b). Moreover, swapping the NTD+linker region between NR2A and NR2B reversed their pH sensitivities, while grafting the NR2A NTD+linker region onto NR2D decreased its proton sensitivity close to that of NR2Awt-containing receptors (Fig. 3b). Proton sensitivity was also decreased when locking open the NR2B-Y282C NTD with MTS-PtrEA (Fig. 3c). Hence, the NR2 dependence of pH sensitivity is unlikely to result from an intrinsic difference in the proton sensor between NR1/NR2 receptor subtypes, but rather from differential access to the proton binding-site owing to the NR2-NTD influence on channel activity.

Our study reveals that the large differences in channel activity conferred by the various NR2 NMDAR subunits originate from a region remote from the agonist-binding/channel gating core. This region comprises the large NR2-NTD and the short linker connecting the NR2-NTD to the ABD. The bilobate NR2-NTD oscillates spontaneously between open-cleft and closed-cleft conformations (Fig. 4), the latter triggering disruption of the ABD dimer interface and subsequent channel closure²⁰. The NTD-ABD linker could exert its key influence by tuning the equilibrium between the different conformations of the NR2-NTD. The identity of the NR2-NTD+linker region also determines the sensitivity to zinc and protons, two endogenous allosteric inhibitors of NMDARs that are likely to be critical in the regulation of NMDAR activity under physiological and pathological conditions^{1,3}. Through its dynamic conformational equilibrium, the NR2-NTD could serve as a target for either negative or positive subunit-specific allosteric modulators (Fig. 4). Compounds like ifenprodil, which bind the NTD cleft and promote its closure (NTD “closers”), behave as subunit-specific NMDAR inhibitors and show good efficacy as neuroprotectants². We propose that molecules that bind the same cleft but impede its closure (NTD “openers”) would behave as NMDAR potentiators (Fig. 4). Such molecules may prove of significant therapeutic benefit, given the accumulating evidence that major human psychoses, including schizophrenia, are associated with a deficit of NMDAR activity^{2,29}.

METHODS SUMMARY

cDNA constructs and site-directed mutagenesis

The pcDNA3-based expression plasmids, mutagenesis and sequencing procedure have been described previously¹⁹. Chimeras were obtained by classical PCR amplification and subsequent subcloning into the parental clone.

Electrophysiology

Recombinant NMDARs were expressed in *Xenopus laevis* oocytes after co-injection of cDNAs (at 10 ng/μl; nuclear injection) coding for the various NR1 and NR2 subunits (ratio

1:1). Oocytes were prepared, injected, voltage-clamped and superfused as described previously¹². Single-channels were recorded from HEK cell outside-out patches.

Methods

Two electrode voltage-clamp recordings and analysis

For all experiments, except for those aimed at measuring pH sensitivity, the standard external solution contained (in mM): 100 NaCl, 2.5 KCl, 0.3 BaCl₂, 5 HEPES (pH 7.3). To chelate trace amounts of contaminant zinc, DTPA (10 μM) was added in all the “0” zinc solutions³¹. For free zinc concentrations in the 1 nM–1 μM range, tricine (10 mM) was used to buffer zinc, while ADA (1 mM) was used to buffer zinc in the 0.1–100 nM range²⁰. For the pH sensitivity experiments, an enriched HEPES external solution was used to insure proper pH buffering²⁰. Currents were elicited by co-application of saturating concentrations of glutamate and glycine (100 μM each), and measured at a holding potential of –60 mV. MTS compounds were used at 0.2 mM (except for Fig. S7). Experiments were done at room temperature. Data collection and analysis of pH and zinc dose-response curves were performed according to ref²⁰. MK-801 time constants of inhibition were obtained by fitting currents with a monoexponential component within a window corresponding to 10%–90% of the maximal inhibition. Data points used for statistical tests were supposed log-normally distributed prior to a Student’s t-test (unless otherwise indicated).

Single-channel recordings and analysis

HEK cells were transfected with 2 μg of cDNAs mixed at a ratio of 1 NR1:3 NR2:3 GFP using calcium phosphate precipitation or FuGENE Transfection Reagent (Roche). Positive cells were visualized by GFP epi-fluorescence. Patch pipettes of 5–10 MΩ were filled with a solution containing (in mM): 115 CsF, 10 CsCl, 10 HEPES, 10 EGTA (pH 7.15 with CsOH). Osmolality was 270 mosm/kg. The standard external solution contained (in mM): 140 NaCl, 2.8 KCl, 0.5 CaCl₂, 10 HEPES, 0.01 EDTA (pH 7.3 with NaOH). Osmolality was adjusted to 290 mosm/kg with sucrose. EDTA was added to chelate trace amounts of contaminant zinc³¹. Channel openings were activated by 100 μM glycine, with 0.05 or 0.01 μM glutamate in most experiments, or with 100 μM glutamate in some patches (included only if no double openings were observed). The holding potential (after correction for junction potential) was –80 to –90 mV. Experiments were performed at room temperature. Currents were recorded with an Axopatch 200B amplifier (Molecular Devices), sampled at 20 to 50 kHz, low-pass filtered (8-pole Bessel) at 5 to 10 kHz. Prior to analysis of P_{open} within a burst, data were digitally refiltered to give a cascaded low-pass filter cutoff frequency of 2 kHz. pClamp 9 or 10 (Molecular Devices) was used to acquire and analyze the data.

The principal goal of single-channel analysis was to measure the open probability (P_{open}) within bursts of channel openings, which provides a good estimate of the P_{open} within an NMDAR activation^{6,32,33}. To idealize single-channel data, transitions were detected using a 50% threshold criterion³⁴. Events of 200 μs duration were excluded from analysis. Missing and ignoring brief events can significantly influence dwell-time histograms. However, such brief events contribute only a tiny fraction of the total time that a channel spends open or closed. Thus, missed events should not have significantly affected measurements of P_{open}. Histograms are presented as square root vs. log time plots³⁵. Shut-time histograms were fitted with 3 or 4 exponential components. A burst was defined as a series of openings separated by closures of duration less than a critical duration, T_{crit}. Bursts with two levels of openings were discarded. We calculated T_{crit} between the two longest components of the shut-time histograms so that total number of event misclassifications is minimized^{34,36}. For NR1wt/NR2Awt and NR1wt/NR2B-(2A NTD+L) receptors, the two longest components of the shut-time distribution differed by a mean factor

> 390, while these components were less separated for NR1wt/NR2Bwt and NR1wt/NR2A-(2B NTD+L) (23-fold and 54-fold separation, respectively). For the latter two constructs, the separation between shut-time components results in a greater than desired number of misclassification of shut times³⁴. This may have led to an overestimation of the P_{open} within a burst. However, for wild-type receptors, our data are overall consistent with previous results^{6,33}, suggesting that our P_{open} estimates are reliable.

Chemicals

HEPES, L-glutamate, glycine, DTPA, EDTA, tricine and ADA were obtained from Sigma, D-APV from Ascent Scientific, 2-aminoethylmethanesulfonatehydrobromide (MTSEA), [2-(trimethylammonium)ethyl]methanesulfonatebromide (MTSET) and 3-(triethylammonium)propylmethanesulfonatebromide (MTS-PtrEA) from Toronto Research Chemicals, (+)MK-801 from Tocris. MTS compounds were prepared as 40 mM stock solutions in bi-distilled water, aliquoted in small volumes (50 μ L) and stored at -20°C ; aliquots were thawed just before use.

Construction of Figure 4

The molecular architecture shown in figure 4a was illustrated by the crystal structure of the mGluR1 ligand-binding domain dimer (pdb 1ewv, ref³⁷) at the level of the NTD, the NMDAR NR1/NR2A agonist-binding domain dimer (pdb 2a5T, ref³⁰) and two subunits of the KcsA tetramer (pdb 1bl8, ref³⁸) as the transmembrane region of the receptor. The fourth transmembrane segment and the C-terminal cytoplasmic region are lacking in this structural depiction.

Supplementary Material

Refer to Web version on PubMed Central for supplementary material.

Acknowledgments

This work was supported by Ministère de la Recherche (MG, LM), UPMC and FRM (MG), NIH grant R01 MH045817 (JWJ), INSERM, ANR, GlaxoSmithKline and Equipe FRM grant (PP). We thank Boris Barbour, Pierre-Jean Corringer, Jacques Neyton and David Stroebel for comments on the manuscript; Stéphanie Carvalho, Mariano Casado and Marie Gendrel for experimental help.

References

1. Dingledine R, Borges K, Bowie D, Traynelis SF. The glutamate receptor ion channels. *Pharmacol Rev.* 1999; 51:7–61. [PubMed: 10049997]
2. Kemp JA, McKernan RM. NMDA receptor pathways as drug targets. *Nat Neurosci.* 2002; 5(Suppl): 1039–1042. [PubMed: 12403981]
3. Paoletti P, Neyton J. NMDA receptor subunits: function and pharmacology. *Curr Opin Pharmacol.* 2007; 7:39–47. [PubMed: 17088105]
4. Cull-Candy SG, Leszkiewicz DN. Role of distinct NMDA receptor subtypes at central synapses. *Sci STKE.* 2004; 2004:re16. [PubMed: 15494561]
5. Chen N, Luo T, Raymond LA. Subtype-dependence of NMDA receptor channel open probability. *J Neurosci.* 1999; 19:6844–6854. [PubMed: 10436042]
6. Erreger K, Dravid SM, Banke TG, Wyllie DJ, Traynelis SF. Subunit-specific gating controls rat NR1/NR2A and NR1/NR2B NMDA channel kinetics and synaptic signalling profiles. *J Physiol.* 2005; 563:345–358. [PubMed: 15649985]
7. Wyllie DJ, Behe P, Colquhoun D. Single-channel activations and concentration jumps: comparison of recombinant NR1a/NR2A and NR1a/NR2D NMDA receptors. *J Physiol.* 1998; 510(Pt 1):1–18. [PubMed: 9625862]

8. Dravid SM, Prakash A, Traynelis SF. Activation of recombinant NR1/NR2C NMDA receptors. *J Physiol.* 2008; 586:4425–4439. [PubMed: 18635641]
9. Popescu G, Robert A, Howe JR, Auerbach A. Reaction mechanism determines NMDA receptor response to repetitive stimulation. *Nature.* 2004; 430:790–793. [PubMed: 15306812]
10. Liu Y, et al. NMDA receptor subunits have differential roles in mediating excitotoxic neuronal death both in vitro and in vivo. *J Neurosci.* 2007; 27:2846–2857. [PubMed: 17360906]
11. Liu L, et al. Role of NMDA receptor subtypes in governing the direction of hippocampal synaptic plasticity. *Science.* 2004; 304:1021–1024. [PubMed: 15143284]
12. Paoletti P, et al. Molecular organization of a zinc binding N-terminal modulatory domain in a NMDA receptor subunit. *Neuron.* 2000; 28:911–925. [PubMed: 11163276]
13. Low CM, Zheng F, Lyuboslavsky P, Traynelis SF. Molecular determinants of coordinated proton and zinc inhibition of N-methyl-D-aspartate NR1/NR2A receptors. *Proc Natl Acad Sci U S A.* 2000; 97:11062–11067. [PubMed: 10984504]
14. Choi YB, Lipton SA. Identification and mechanism of action of two histidine residues underlying high-affinity Zn²⁺ inhibition of the NMDA receptor. *Neuron.* 1999; 23:171–180. [PubMed: 10402203]
15. Perin-Dureau F, Rachline J, Neyton J, Paoletti P. Mapping the binding site of the neuroprotectant ifenprodil on NMDA receptors. *J Neurosci.* 2002; 22:5955–5965. [PubMed: 12122058]
16. Jones KS, VanDongen HM, VanDongen AM. The NMDA receptor M3 segment is a conserved transduction element coupling ligand binding to channel opening. *J Neurosci.* 2002; 22:2044–2053. [PubMed: 11896144]
17. Yuan H, Erreger K, Dravid SM, Traynelis SF. Conserved structural and functional control of N-methyl-D-aspartate receptor gating by transmembrane domain M3. *J Biol Chem.* 2005; 280:29708–29716. [PubMed: 15970596]
18. Blanke ML, VanDongen AM. Constitutive activation of the N-methyl-D-aspartate receptor via cleft-spanning disulfide bonds. *J Biol Chem.* 2008; 283:21519–21529. [PubMed: 18450751]
19. Rachline J, Perin-Dureau F, Le Goff A, Neyton J, Paoletti P. The micromolar zinc-binding domain on the NMDA receptor subunit NR2B. *J Neurosci.* 2005; 25:308–317. [PubMed: 15647474]
20. Gielen M, et al. Structural rearrangements of NR1/NR2A NMDA receptors during allosteric inhibition. *Neuron.* 2008; 57:80–93. [PubMed: 18184566]
21. Sun Y, et al. Mechanism of glutamate receptor desensitization. *Nature.* 2002; 417:245–253. [PubMed: 12015593]
22. Mayer ML. Glutamate receptors at atomic resolution. *Nature.* 2006; 440:456–462. [PubMed: 16554805]
23. Tang C, Schwieters CD, Clore GM. Open-to-closed transition in apo maltose-binding protein observed by paramagnetic NMR. *Nature.* 2007; 449:1078–1082. [PubMed: 17960247]
24. Kniazeff J, et al. Locking the dimeric GABA(B) G-protein-coupled receptor in its active state. *J Neurosci.* 2004; 24:370–377. [PubMed: 14724235]
25. Mony L, et al. Structural basis of NR2B-selective antagonist recognition by N-methyl-D-aspartate receptors. *Mol Pharmacol.* 2009; 75:60–74. [PubMed: 18923063]
26. Zheng F, et al. Allosteric interaction between the amino terminal domain and the ligand binding domain of NR2A. *Nat Neurosci.* 2001; 4:894–901. [PubMed: 11528420]
27. Marvin JS, Hellinga HW. Manipulation of ligand binding affinity by exploitation of conformational coupling. *Nat Struct Biol.* 2001; 8:795–798. [PubMed: 11524684]
28. Low CM, et al. Molecular determinants of proton-sensitive N-methyl-D-aspartate receptor gating. *Mol Pharmacol.* 2003; 63:1212–1222. [PubMed: 12761330]
29. Lisman JE, et al. Circuit-based framework for understanding neurotransmitter and risk gene interactions in schizophrenia. *Trends Neurosci.* 2008; 31:234–242. [PubMed: 18395805]
30. Furukawa H, Singh SK, Mancusso R, Gouaux E. Subunit arrangement and function in NMDA receptors. *Nature.* 2005; 438:185–192. [PubMed: 16281028]
31. Paoletti P, Ascher P, Neyton J. High-affinity zinc inhibition of NMDA NR1-NR2A receptors. *J Neurosci.* 1997; 17:5711–5725. [PubMed: 9221770]

32. Erreger K, Traynelis SF. Zinc inhibition of rat NR1/NR2A N-methyl-D-aspartate receptors. *J Physiol.* 2008; 586:763–778. [PubMed: 18048453]
33. Schorge S, Elenes S, Colquhoun D. Maximum likelihood fitting of single channel NMDA activity with a mechanism composed of independent dimers of subunits. *J Physiol.* 2005; 569:395–418. [PubMed: 16223763]
34. Colquhoun, D.; Sigworth, FJ. *Single-Channel Recording.* Sakmann, B.; Neher, E., editors. New York: Plenum Press; 1995. p. 483-587.
35. Sigworth FJ, Sine SM. Data transformations for improved display and fitting of single-channel dwell time histograms. *Biophys J.* 1987; 52:1047–1054. [PubMed: 2447968]
36. Jackson MB, Wong BS, Morris CE, Lecar H, Christian CN. Successive openings of the same acetylcholine receptor channel are correlated in open time. *Biophys J.* 1983; 42:109–114. [PubMed: 6301575]
37. Kunishima N, et al. Structural basis of glutamate recognition by a dimeric metabotropic glutamate receptor. *Nature.* 2000; 407:971–977. [PubMed: 11069170]
38. Doyle DA, et al. The structure of the potassium channel: molecular basis of K⁺ conduction and selectivity. *Science.* 1998; 280:69–77. [PubMed: 9525859]

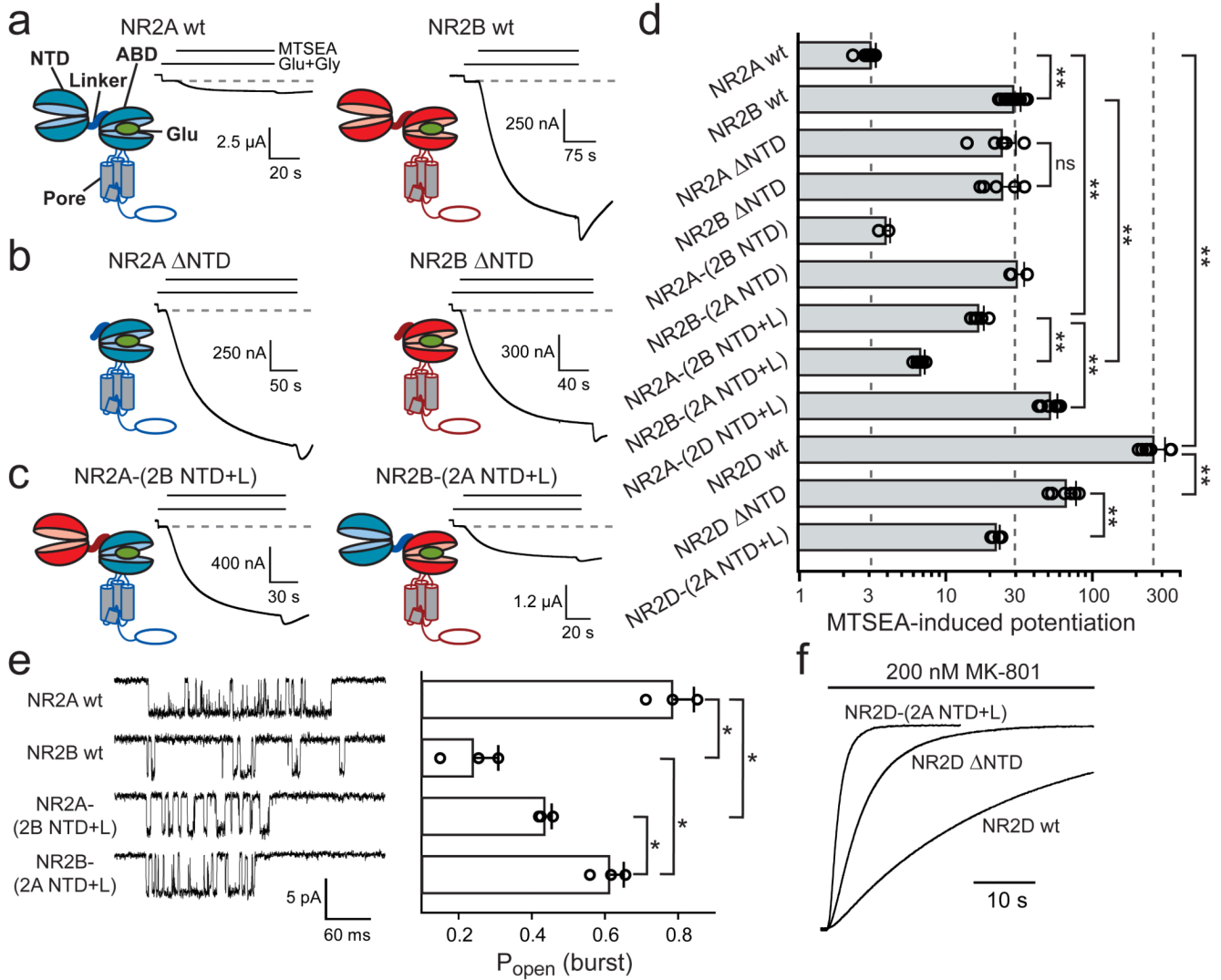


Figure 1. The NR2 NTD+linker region controls NMDAR P_o

a–c Potentiation by MTSEA of receptors incorporating NR1-A652C and the indicated NR2 subunits. NTD, N-terminal domain; ABD, agonist-binding domain. **d** Pooled data (mean \pm s.d.), from top to bottom: 3.2 \pm 0.3 (n=12), 30 \pm 4 (n=14), 25 \pm 6 (n=6), 25 \pm 7 (n=5), 4.0 \pm 0.3 (n=3), 32 \pm 4 (n=3), 17 \pm 2 (n=6), 6.9 \pm 0.5 (n=5), 53 \pm 7 (n=9), 270 \pm 60 (n=7), 68 \pm 12 (n=6) and 23 \pm 2 (n=5) (**p < 0.001). **e** P_o within bursts of openings for receptors incorporating NR1wt and the indicated NR2 subunit. Left: representative traces of bursts. Right (from top to bottom): 0.78 \pm 0.06 (n=3), 0.24 \pm 0.07 (n=3), 0.43 \pm 0.02 (n=3) and 0.61 \pm 0.04 (n=3) (*p < 0.05, Student's t-test). **f** Kinetics of inhibition by MK-801 at receptors incorporating NR1wt and NR2Dwt (τ_{on} = 32 s), NR2D- Δ NTD (5.7 s) or NR2D-(2A NTD+L) (1.6 s). Error bars represent s.d.

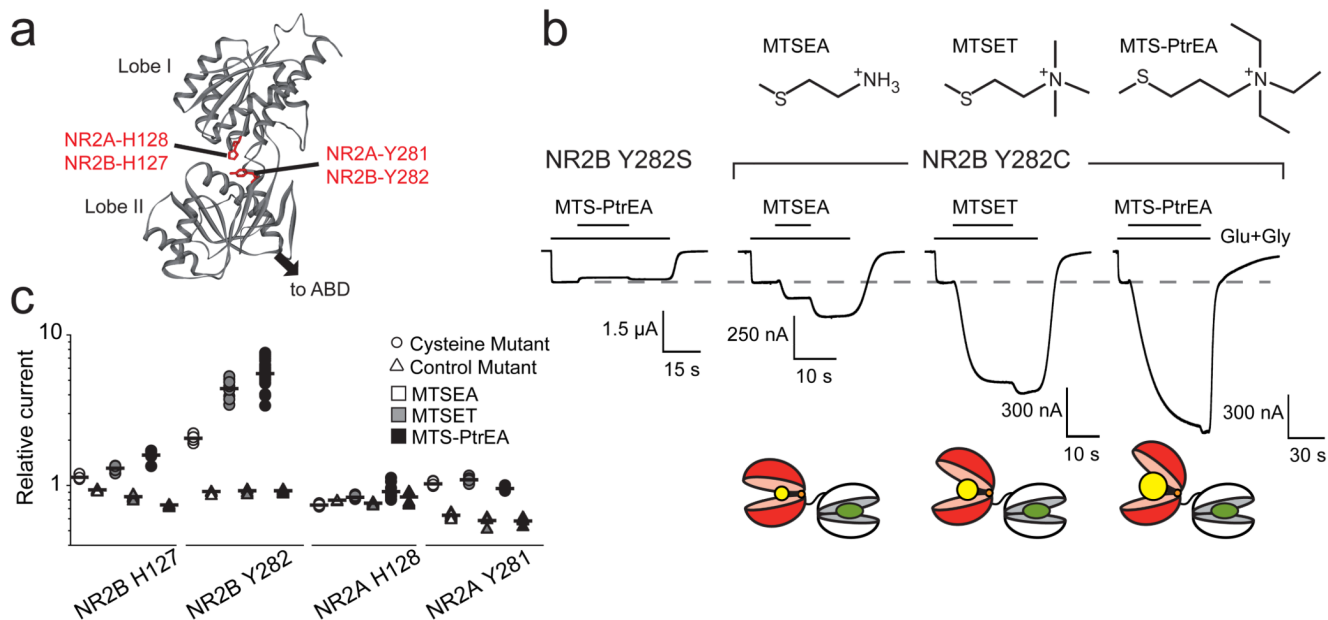


Figure 2. Locking open the NR2-NTD increases NMDAR activity

a 3D model of NR2B-NTD. **b** Top: chemical formula of the transferable moiety of MTSEA, MTSET and MTS-PtrEA. Middle: Recordings from NR1wt/NR2B-Y282C and control NR1wt/NR2B-Y282S receptors during MTS treatment. The potentiation upon MTS wash likely reflects the washout of a reversible pore-blocking effect of the positively charged MTS. Bottom: Schematic representations of the NTD-ABD tandem of NR2B-Y282C after MTS-modification (MTS head group in yellow). **c** Relative currents after application of MTSEA, MTSET and MTS-PtrEA to receptors incorporating NR1wt and the indicated NR2 subunit. See Table S1 for values.

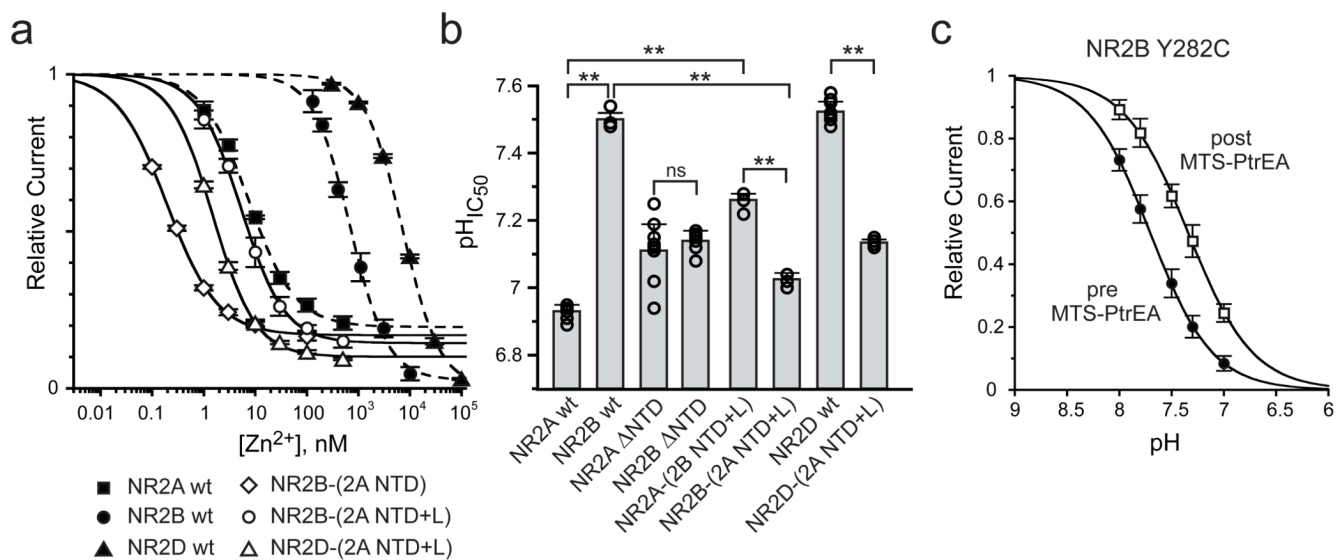


Figure 3. The NR2 NTD+linker region controls zinc and proton sensitivities of NMDARs

a Zinc sensitivity of receptors incorporating NR1wt and (Inhib_{max}, IC₅₀): NR2Awt (81%, 7.5 nM [n=6]), NR2Bwt (98%, 720 nM [n = 13]), NR2Dwt (100%, 7.8 μM [n=3]), NR2B-(2A NTD) (83%, 0.20 nM [n=4]), NR2B-(2A NTD+L) (86%, 5.4 nM [n=4]) or NR2D-(2A NTD+L) (90%, 1.5 nM [n=5]). n_H in the 0.9–1.2 range. **b** pH_{IC50} of receptors incorporating NR1wt and the indicated NR2 subunit. See Table S2 for values. (**p<0.001). **c** Proton sensitivity of NR1wt/NR2B-Y282C receptors before (pH_{IC50} = 7.70, n_H = 1.5 [n=3]) and after (pH_{IC50} = 7.34, n_H = 1.4 [n=3]) MTS-PtrEA modification. Error bars represent s.d.

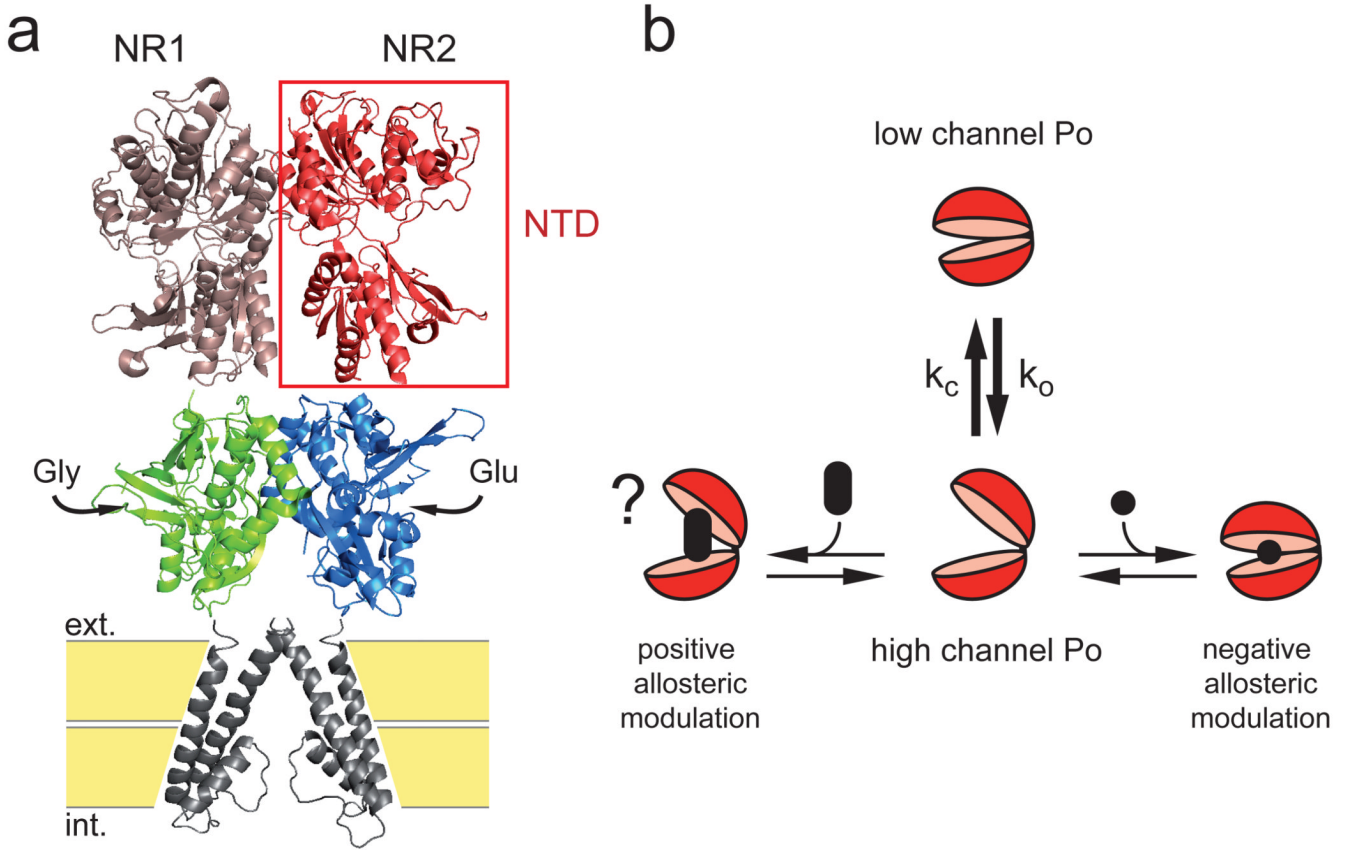


Figure 4. Model for the control of NMDAR activity by the NR2 N-terminal domain
a Structural depiction of an NMDAR. The full receptor is a tetramer but only a NR1/NR2 dimer is shown³⁰. **b** In its ligand-free state, the NR2-NTD alternates between open- and closed-cleft conformations, the latter favoring pore closure. In the model, this equilibrium determines the subtype-specificity of NMDAR P_o ($k_o/k_c[\text{NR2B}] < k_o/k_c[\text{NR2A}]$). The NTD is also the target of subunit-specific allosteric inhibitors such as zinc^{12–14,19} or ifenprodil^{15,25}, which bind the NTD central cleft and promote domain closure. We hypothesize that a molecule binding in the same cleft, but preventing its closure, behaves as a positive allosteric modulator, enhancing receptor activity.